



**HAL**  
open science

## Controlled diffusion by thin layer coating: The intricate case of the glass-stopper interface

Julie Chanut, Jean-Pierre Bellat, Régis Gougeon, Thomas Karbowski

### ► To cite this version:

Julie Chanut, Jean-Pierre Bellat, Régis Gougeon, Thomas Karbowski. Controlled diffusion by thin layer coating: The intricate case of the glass-stopper interface. *Food Control*, 2021, 120, pp.107446. 10.1016/j.foodcont.2020.107446 . hal-02989078

**HAL Id: hal-02989078**

**<https://institut-agro-dijon.hal.science/hal-02989078v1>**

Submitted on 24 Aug 2022

**HAL** is a multi-disciplinary open access archive for the deposit and dissemination of scientific research documents, whether they are published or not. The documents may come from teaching and research institutions in France or abroad, or from public or private research centers.

L'archive ouverte pluridisciplinaire **HAL**, est destinée au dépôt et à la diffusion de documents scientifiques de niveau recherche, publiés ou non, émanant des établissements d'enseignement et de recherche français ou étrangers, des laboratoires publics ou privés.



Distributed under a Creative Commons Attribution - NonCommercial 4.0 International License

# Controlled diffusion by thin layer coating: the intricate case of the glass-stopper interface

*Julie Chanut*<sup>a,b</sup>, *Jean-Pierre Bellat*<sup>b</sup>, *Régis D. Gougeon*<sup>a,c</sup>, *Thomas Karbowski*<sup>a,\*</sup>

<sup>a</sup> Univ. Bourgogne Franche-Comté, Agrosup Dijon, PAM UMR 02 102, 1 Esplanade Erasme, 21000 Dijon, France

<sup>b</sup> Univ. Bourgogne Franche-Comté, Laboratoire Interdisciplinaire Carnot de Bourgogne, UMR 6303 CNRS, 9 Avenue Alain Savary, 21000 Dijon, France

<sup>c</sup> Univ. Bourgogne Franche-Comté, Institut Universitaire de la Vigne et du Vin, 1 rue Claude Ladrey, 21000 Dijon, France

## **Corresponding Author:**

Prof. Thomas Karbowski, Univ. Bourgogne Franche-Comté, AgroSup Dijon, PAM UMR 02 102, 1 Esplanade Erasme, 21000 Dijon, France, phone number: +33380772388,

\* E-mail: [thomas.karbowski@agrosupdijon.fr](mailto:thomas.karbowski@agrosupdijon.fr)

22 ABSTRACT

23  
24 A comprehensive study was carried out to investigate the critical role played by the interface  
25 between the stopper and the bottleneck on oxygen penetration into the bottle, as well as the effect  
26 of surface treatment of the stopper. First, the compression of micro-agglomerated cork, at close to  
27 40% (similar to that of a cork stopper in a still wine bottleneck), had a very limited effect on the  
28 oxygen transfer. Second, once a cork was inserted into a glass bottleneck without any surface  
29 treatment, up to 99% of the total oxygen transfer took place at the stopper-bottleneck interface.  
30 Third, when the cork surface was coated with a paraffin-silicone mixture, there was almost no  
31 oxygen transfer at the interface. Although initially used as a slippery agent for easier uncorking,  
32 the surface coating of the stopper, as a thin layer of several hundred nanometers, had a  
33 remarkable and unexpected impact on the control of the oxygen transfer.

34  
35  
36

37 **KEYWORDS** gas transfer, oxygen, agglomerated cork, interface, surface treatment.

38  
39  
40  
41  
42  
43  
44  
45  
46  
47  
48

## 1. INTRODUCTION

49  
50  
51 During wine conservation in a bottle, the control of oxygen transfer from the outside environment  
52 to the wine inside the bottle is a key parameter that determines the wine quality. Many other  
53 factors can also influence the evolution of wine during postbottling aging, such as the  
54 composition of the wine itself (also related to the wine-making process), the temperature, the  
55 relative humidity, the storage position, as well as the amount of oxygen initially present in the  
56 bottle (Arapitsas et al., 2014; Lopes, Saucier, Teissedre & Glories, 2006; Lopes et al., 2012;  
57 Roullier-Gall et al., 2017; Venturi et al., 2016). However, the oxygen transfer is the most critical  
58 factor (Roullier-Gall et al., 2016). For this reason, the choice of the packaging and in particular of  
59 the stopper is crucial in providing the best conditions for wine aging (Caloghiris, Waters &  
60 Williams, 1997; Crouvisier-Urien, Bellat, Gougeon & Karbowiak, 2018; Karbowiak et al., 2010;  
61 Lopes, Saucier, Teissedre & Glories, 2007a; Lopes, Saucier, Teissedre & Glories, 2007b; Waters,  
62 Peng, Pocock & Williams, 1996).

63 The transfer of oxygen into the bottle occurs by diffusion through the stopper itself and also at  
64 the interface between the glass bottleneck and the cork stopper. The oxygen transfer at the  
65 interface between the glass bottleneck and the cork stopper was first investigated experimentally  
66 in two studies (Lopes, Saucier, Teissedre & Glories, 2007b; Waters et al., 2001). Lopes *et al.* and  
67 Waters *et al.* measured the oxygen transfer through cork stoppers compressed in a bottleneck  
68 with an epoxy glue applied to the stopper-bottleneck interface present on the external surface in  
69 contact with the air. Their setup prevented the entry of oxygen through this top part of the cork-  
70 glass interface but still allowed the transfer that can occur through the lower part of the stopper-  
71 bottleneck interface once it has passed through the outer surface. A preliminary study by  
72 Lagorce-Tachon *et al.*, on natural cork stopper inserted in a bottleneck without surface treatment

73 showed that the global diffusion coefficient through the cork-glass bottleneck system was fifty  
74 times higher ( $5 \times 10^{-7} \text{ m}^2.\text{s}^{-1}$ ) than through the compressed cork stopper alone ( $8 \times 10^{-9} \text{ m}^2.\text{s}^{-1}$ )  
75 (Lagorce-Tachon et al., 2016).

76 Recently, Karbowskiak *et al.* measured the oxygen transfer through corked bottlenecks and through  
77 cork stoppers alone for bottles containing oxidized and nonoxidized white wines (Karbowskiak et  
78 al., 2019). Their results showed that the effective oxygen diffusion coefficient for the cork  
79 compressed in a bottleneck was considerably higher for oxidized wines than for nonoxidized  
80 wines, whereas the oxygen diffusion coefficient for the cork stopper alone remained similar in all  
81 cases. However, in the studies by Lagorce-Tachon *et al.* and Karbowskiak *et al.*, the diffusion  
82 coefficient values were measured on dry cork without taking into account the possible effects of  
83 water and ethanol on barrier and mechanical properties of cork. These two studies highlight that  
84 the cork stopper-glass bottleneck interface is likely to play an important role in oxygen transfer.

85 With the various types cork stopper currently used (natural or agglomerated), an additional outer  
86 layer of a surface treatment product is always applied in the final step of the manufacturing  
87 process. The most common coating agents are food-grade paraffin wax, silicone, or emulsions of  
88 these two products in a mixture (Lefebvre et al., 2006). They are usually spread in a drum coater  
89 to cover the surface of the stoppers, but the method of application and the quantity applied  
90 depend on the cork supplier. The primary function of these surface treatments is to facilitate the  
91 introduction and especially the extraction of the stopper from the bottleneck at the opening as  
92 they reduce the adhesion between the glass and the cork acting as a slippery agent (Chatonnet &  
93 Labadie, 2003; Fortes, Rosa & Pereira, 2004; Gonzalez-Adrados et al., 2011). They also improve  
94 the tightness to liquids by reducing the risk of leakage and they reduce the kinetics of liquid  
95 sorption by the stopper during cork-wine interaction (Gonzalez-Adrados et al., 2008). However,

96 only a few studies have reported the effect of the coating agents on the transfer of oxygen through  
97 the cork-bottleneck system (Keenan, Gozukara, Christie & Heyes, 1999; Waters, 1997).  
98 Keenan *et al.* determined the oxygen permeability of macrocrystalline paraffin wax coated on  
99 natural cork stoppers and calculated the theoretical ingress of oxygen diffusing through a 17  $\mu\text{m}$   
100 layer of macrocrystalline paraffin wax coated on these stoppers. The oxygen transfer through the  
101 paraffin layer was not sufficient to cause the wine oxidation. The calculation was made in the  
102 case of a continuous coating along the stopper compressed in a cylindrical tube (18.5 mm in  
103 diameter) and did not take into account the permeation of oxygen along the interface between the  
104 bottleneck and cork coating. Therefore, it is particularly relevant to investigate the oxygen  
105 transfer through the system composed of a cork stopper that has undergone a surface treatment  
106 prior to being inserted in a glass bottleneck.

107  
108 The present work examines the oxygen transfer at the interface between the glass bottleneck and  
109 the cork stopper. In particular, we focus on the effect of surface treatment of the stopper on the  
110 oxygen transfer at the glass-stopper interface. First, permeation experiments were performed for  
111 uncompressed and compressed (40% in volume) micro-agglomerated stoppers to determine their  
112 intrinsic oxygen diffusion coefficients and the effect of compression. Then, permeation  
113 experiments were carried out on the system composed of the cork stopper without surface  
114 treatment inserted in a glass bottleneck. In the final step, the oxygen transfer was evaluated on the  
115 glass-stopper system with the stopper coated with a surface treatment product. This  
116 comprehensive approach aimed to quantify and differentiate between the two oxygen flows  
117 passing through the stopper and at the interface between the stopper and the glass.

118

119

120       2. MATERIALS AND METHODS

121

122       **2.1. Cork stopper samples**

123       Micro-agglomerated cork stoppers (of the type Diam 10) were produced by Diam Bouchage  
124       (Céret, France) by a molding process using cork particles associated with binding agents. The  
125       stoppers used for the experiments were 24.2 mm in diameter and 49 mm long and were either  
126       coated with an anionic emulsion of paraffin and silicone or were without a surface treatment  
127       agent. The different conditions used are summarized in figure 1.

128       2.1.1. Compressed cork stopper

129       Cork wafers 3 mm thick were cut in the middle of full-length cork stoppers. They were then  
130       inserted uncompressed in a metal ring and attached at the periphery with Araldite 2012 to avoid  
131       gas transfer at the interface. The experiments were carried out on 3 mm thick cork wafers to  
132       reduce the time of measurement.

133       2.1.2. Compressed cork stopper

134       Full-length cork stoppers were first compressed using a professional bottling machine comprising  
135       four stainless steel jaws (GAI 4040, France) and inserted in a metal ring of 18.5 mm diameter,  
136       corresponding to the diameter of the entry bore of a bottleneck (AFNOR, 2018). This operation  
137       leads to a 40% compression of the initial stopper volume. Similar to uncompressed cork stoppers,  
138       the interface between the cork wafer and the metal ring was glued to avoid gas transfer at the  
139       interface. Here, the cork samples were 6 mm thick to prevent buckling during compression.

140       2.1.3. Cork stopper inserted in a glass bottleneck

141       Uncoated full-length cork stoppers were inserted in empty glass bottles (Bourgogne Astre 37.5  
142       cL, Verrerie de Bourgogne, France) using the same bottling machine. Prior to bottling, the

143 bottleneck profile of each bottle was measured using a profilometer (Egitron PerfiLab PRF 2014  
144 01) to ensure they complied with the corresponding standard (AFNOR, 2018). The bottles were  
145 then cut below the stopper with a diamond cutoff wheel and inserted in a metal ring (Figure 2).  
146 Here, only the part between the ring and the bottleneck was glued with Araldite 2012. Oxygen  
147 transfer measurements were performed on 49-mm-long closures inserted in a bottleneck having  
148 an inner diameter of  $18.5 \pm 0.5$  mm.

#### 149 2.1.4. Cork stopper with surface coating

150 The same procedure was applied for cork stoppers coated with a surface treatment product. A  
151 coating composed of an emulsion of paraffin wax and silicone was sprayed in a drum coater at an  
152 industrial scale. For these stoppers, only 6 mm wafers were inserted in the bottleneck (Figure 2).  
153 This allowed the time of permeation experiment to be reduced. Ten measurements were  
154 performed for each of the four conditions chosen for this comprehensive study.

## 155 2.2. Oxygen permeation

157 During storage, we can distinguish between two phenomena; the oxygen given out by the stopper  
158 expressed by the oxygen initial release (OIR), and the oxygen coming from the outside  
159 environment expressed by the oxygen transmission rate (OTR) (Chevalier, Pons & Loisel, 2019).  
160 In this study, the OTR was determined using a homemade apparatus based on a manometric  
161 method (Figure 2).

162 The equipment and protocol have been detailed previously (Lagorce-Tachon et al., 2014; Lequin  
163 et al., 2012). The oxygen flow was measured through a sample separating two chambers. First, an  
164 oxygen purge was performed in the measuring chamber  $C_1$ . The initial pressure was then set at  
165 around 900 hPa while the other compartment,  $C_2$ , was kept under dynamic vacuum (0.1 hPa).



166 The decrease in oxygen pressure in the measuring compartment, caused by the transfer of oxygen  
167 from compartment C<sub>1</sub> to, C<sub>2</sub> was monitored over time. The temperature was kept constant at 298  
168 K (±1 K) by a water circulation surrounding compartment C<sub>1</sub> under thermostat control. The  
169 pressure sensitivity was ± 0.1 hPa.

170

### 171 **2.3. Scanning electron microscopy**

172 Prior to bottling, agglomerated cork stoppers without and with surface treatment were observed  
173 by SEM using a Jeol JSM 7600F apparatus (3.5 kV). Before imaging, cork samples were cut with  
174 a razor blade, and coated with a carbon film (15–20 nm). The obtained images allowed us to  
175 visualize the distribution of the surface treatment product on the stopper surface as well as the  
176 thickness of the coating.

## 177 **3. CALCULATION**

178

### 179 **3.1. Oxygen transfer in the cork stopper**

180 Considering the gas as ideal, the surface molar flow of oxygen passing through the wafer, J<sub>w</sub>  
181 (mol.m<sup>-2</sup>.s<sup>-1</sup>) is given by the equation:

182

$$183 \quad J_w = -\frac{1}{S_w} \frac{dn}{dt} = -\frac{V}{S_w \cdot R \cdot T} \frac{dp}{dt} \quad (\text{Equation 1})$$

184

185  $p$  is the pressure (Pa) in the compartment C<sub>1</sub> along time  $t$  (s),  $V$  is the volume of the compartment  
186 C<sub>1</sub> (m<sup>3</sup>),  $S_w$  is the surface of the wafer (m<sup>2</sup>),  $R$  is the ideal gas constant (8.314 J. mol<sup>-1</sup>.K<sup>-1</sup>) and  $T$   
187 is the temperature (K).

188 According to the first Fick's law, the surface molar flow of oxygen passing through the cork  
189 wafer, once the steady state is established, is also given by the equation:

190 
$$J_w = -D_w \cdot \nabla C^a \approx -D_w \cdot \frac{C^a}{e} \quad (\text{Equation 2})$$

191 With  $D_w$  the diffusion coefficient ( $\text{m}^2 \cdot \text{s}^{-1}$ ) of oxygen inside the wafer,  $e$  the thickness of the wafer  
192 (m) and  $\nabla C^a$  ( $\text{mol} \cdot \text{m}^{-4}$ ) the concentration gradient of oxygen adsorbed on both side of the wafer.  
193  $C^a$  ( $\text{mol} \cdot \text{m}^{-3}$ ) is related to the concentration of the gas  $C^g$  ( $\text{mol} \cdot \text{m}^{-3}$ ) by the equation:

194  
195 
$$C^a = \psi \cdot C^g \quad (\text{Equation 3})$$

196  
197 With  $\psi$ , so called the separation factor.  $\Psi$  is obtained from the sorption isotherm of oxygen, on  
198 cork which has been determined on previous work(Lequin et al., 2012).

199  
200 By combining the equations (1), (2) and (3), and after integration over time, we obtain:

201  
202 
$$\ln \left( \frac{p_{t=0}}{p_t} \right) = \frac{D_w \cdot \psi \cdot S_w}{e \cdot V} \cdot t \quad (\text{Equation 4})$$

203  
204 Thus, the diffusion coefficient of oxygen through the cork wafer is determined from the slope of  
205 the straight-line of the plot  $\ln \left( \frac{p_{t=0}}{p_t} \right) = f(t)$  obtained once the steady state is established.

206  
207

### 208 **3.2. Extrapolation of the diffusion coefficient for a full-length cork stopper**

209 As cork stoppers are not homogeneous materials, the diffusion coefficient measured through a  
210 cork wafer of thickness  $e$  is not representative of the diffusion coefficient through a full-length  
211 cork stopper of length  $L_s$ . For the measurements made on wafers 3 or 6 mm thick, it was thus  
212 necessary to extrapolate the experimental results to a full-length cork stopper. To that end, the  
213 stopper was considered as a serial stack of  $n$  wafers, where each slice represents a local resistance  
214 to gas transfer,  $R_w$ . The sum of these resistances allowed us to calculate the total resistance  $R_s$  of  
215 the stopper, as defined by the following equations:

$$216 \quad R_s = \frac{L_s}{D_s} = \sum_{i=1}^n R_{wi} = \sum_{i=1}^n \frac{e}{D_{wi}} \quad (\text{Equation 5})$$

$$217 \quad L_s = e \cdot n \quad (\text{Equation 6})$$

$$218 \quad \frac{1}{D_s} = \frac{1}{n} \sum_{i=1}^n \frac{1}{D_{wi}} \quad (\text{Equation 7})$$

219 Where  $R_s$  is the overall resistance of the stopper,  $D_s$  is the extrapolated diffusion coefficient of the  
220 stopper,  $L_s$  is the total length of the stopper,  $n$  is the total number of wafers contained in a full-  
221 length stopper and  $D_{wi}$  is the diffusion coefficient of the wafer  $i$  drawn at random in the statistical  
222 distribution of diffusion coefficients determined experimentally.

223

### 224 **3.3. Oxygen transfer at the glass-cork interface**

225 The oxygen flow through the cork stopper-glass bottleneck interface,  $J_{\text{interface}}$  ( $\text{mol}\cdot\text{m}^{-2}\cdot\text{s}^{-1}$ ), is  
226 determined by subtracting from the total flow,  $J_{\text{total}}$ , going through the system comprising the cork  
227 stopper inserted in the glass bottleneck, the oxygen flow going through the cork stopper alone,  $J_s$ .

$$228 \quad J_{\text{interface}} = J_{\text{total}} - J_s \quad (\text{Equation 8})$$

229 The total flow of gas passing through the bottleneck-cork system is expressed by an equation  
230 similar to Equation 1:

$$231 \quad J_{total} = -\frac{1}{S} \frac{dn}{dt} = -\frac{V}{S.R.T} \frac{dp}{dt} \simeq -\frac{V}{S.R.T} \frac{\Delta p}{\Delta t} \text{ (Equation 9)}$$

232 As we know the diffusion coefficient of oxygen through the full-length cork stopper,  $D_s$ , the flow  
233 passing only through the cork stopper is calculated with the relation:

$$234 \quad J_s = -D_s \cdot S \cdot \frac{\Delta p}{L_s.R.T} \text{ (Equation 10)}$$

235 In the last two equations,  $S$  is the section area of the cork inserted in the bottleneck, and  $\Delta p$  is the  
236 pressure decrease in compartment  $C_1$  during time,  $\Delta t$ .

237

## 238 4. RESULTS AND DISCUSSION

239

### 240 4.1. Role of the compression on the oxygen transfer

241 To determine the effect of compression on the gas transfer through the cork stopper, the effective  
242 diffusion coefficient of oxygen was first measured on uncompressed and compressed cork  
243 wafers, with the interface glued in both cases. The experimental and extrapolated oxygen  
244 diffusion coefficient values for the compressed and uncompressed samples are given in Figure 3  
245 and in Table 1. The effective oxygen diffusion coefficient through uncompressed 3 mm cork  
246 wafers was between  $10^{-12} \text{ m}^2.\text{s}^{-1}$  and  $10^{-10} \text{ m}^2.\text{s}^{-1}$ . For the compressed 6 mm cork wafers, the  
247 effective diffusion coefficient values ranged from  $10^{-11}$  to  $10^{-10} \text{ m}^2.\text{s}^{-1}$ . These data were then  
248 extrapolated to a full-length cork stopper (48 mm) for comparison using the model of series  
249 resistances to mass transfer. From the statistical distribution, the oxygen diffusion coefficient

250 value was reduced from  $1.4 \times 10^{-11} \text{ m}^2.\text{s}^{-1}$  for the uncompressed to  $9.2 \times 10^{-12} \text{ m}^2.\text{s}^{-1}$  for the  
251 compressed cork stoppers.

252 Thus, when compression corresponding to a reduction of 40% in volume is applied to the  
253 stopper, this leads to a slight decrease in the oxygen transfer through the stopper with a reduction  
254 of the oxygen diffusion coefficient by a factor of 1.5. With natural cork stoppers, Lagorce-  
255 Tachon *et al.* did not find a significant impact of compression on the diffusion coefficient of  
256 oxygen after a 40% reduction in volume (with a diameter reduction from 24 mm to 18.5  
257 mm)(Lagorce-Tachon et al., 2016). Indeed, the effective diffusion coefficients measured after  
258 compression led to a relatively large distribution of oxygen diffusion coefficients of  
259 uncompressed cork ranging from  $10^{-10}$  to  $10^{-7} \text{ m}^2.\text{s}^{-1}$ . In such a case, it is highly probable that the  
260 heterogeneity between samples of natural cork (which are much more heterogeneous than  
261 agglomerated cork) masked the effect of the compression. For agglomerated cork stoppers, the  
262 statistical distribution of the effective diffusion coefficients for full-length stoppers were  
263 narrowed to values around  $10^{-11} \text{ m}^2.\text{s}^{-1}$ , reflecting the homogeneity of the agglomerated cork  
264 stoppers and indicating the effect of compression on oxygen transfer. These results also accord  
265 with those reported by Rabirot *et al.* They measured oxygen permeability in dry condition for  
266 agglomerated cork wafers (10 mm thick) with the initial diameter of 24 mm compressed to final  
267 diameters of 21 mm and 18.5 mm, which represent the lower and upper bottleneck diameters,  
268 respectively (Rabirot, Sanchez & Aracil, 1999). Such differences in the compression of the  
269 stopper, corresponding to a reduction between 23% and 40% in volume, led to a decrease in  
270 oxygen permeability between  $9.3 \times 10^{-13} \text{ mol.m.m}^{-2}.\text{Pa}^{-1}.\text{s}^{-1}$  and  $1.8 \times 10^{-13} \text{ mol.m.m}^{-2}.\text{Pa}^{-1}.\text{s}^{-1}$ ,  
271 respectively, which represents a reduction in oxygen permeability by a factor of 5. This decrease  
272 in the oxygen transfer through an agglomerated cork stopper could be attributed to a reduction in

273 the initial porosity between cork particles. This could vary according to the formulation of the  
274 agglomerated cork stopper, in particular with respect to the ratio of weight of adhesive to the  
275 weight of cork (Crouvisier-Urien et al., 2020).

#### 276 **4.2. Oxygen transfer at the stopper-bottleneck interface: role of the surface treatment**

277 In the second step, the effective diffusion coefficient of oxygen through the whole stopper-  
278 bottleneck system was determined. First, this was calculated for stoppers with no surface  
279 treatment and then for stoppers coated with an emulsion of paraffin and silicone. This allowed us  
280 to evaluate the gas transfer at the stopper-bottleneck interface and to assess the impact of the  
281 surface treatment on the oxygen diffusion. The experimental and extrapolated distributions of the  
282 logarithm of the diffusion coefficient of oxygen of the different samples are reported in Figure 4  
283 and the mean oxygen diffusion coefficients extrapolated to a full cork stopper are displayed in  
284 Table 1.

285 For the stopper without a surface treatment agent and inserted in the bottleneck, the mean  
286 effective diffusion coefficient appeared significantly higher than that of cork stoppers alone (i.e.,  
287 outside the bottleneck) and with the same compression level. The mean value was  $1.3 \times 10^{-7} \text{ m}^2 \cdot \text{s}^{-1}$   
288 <sup>1</sup> for the former compared with  $9.2 \times 10^{-12} \text{ m}^2 \cdot \text{s}^{-1}$  for the latter. Such a stopper-bottleneck system  
289 is thus much more permeable than a compressed stopper outside the bottleneck (with the  
290 interface glued). The poor resistance to gas transfer of this system must therefore originate from  
291 the stopper-glass interface, which thus addresses the likely role of defects (macropores, scratches,  
292 roughness irregularities, etc.) formed on the cork surface during its processing or at the bottling  
293 stage, or of defects present on the surface of the bottleneck. Such defects might constitute  
294 preferential pathways for gas transfer.

295 The OTRs through the stopper-bottleneck systems and through the stoppers alone were also  
 296 calculated to determine the OTR through the interface. These results are summarized in Table 1  
 297 and highlight that more than 99% of the total oxygen transfer occurs at the stopper-bottleneck  
 298 interface. A similar result was previously found for natural cork with an effective diffusion  
 299 coefficient 50 times higher for a natural whole cork stopper compressed in a bottleneck compared  
 300 with a compressed stopper alone with the interface glued (Lagorce-Tachon et al., 2016).

301 **Table 1.** Mean oxygen diffusion coefficients and OTRs determined for uncompressed and compressed  
 302 cork stoppers alone and for cork stoppers inserted in a bottleneck with and without a surface treatment  
 303 agent (extrapolated to a full cork stopper, from 10 replicates in each case; see figure 4 for corresponding  
 304 distributions). For practical reasons, OTR is expressed as  $\text{mg}\cdot\text{year}^{-1}$ , referring to as mg of oxygen going  
 305 through the stopper per year.

	<b>Effective Diffusion Coefficient <math>D_s</math> (<math>\times 10^{-12} \text{ m}^2\cdot\text{s}^{-1}</math>)</b>	<b>OTR<sub>total</sub> (<math>\text{mg}\cdot\text{year}^{-1}</math>)</b>	<b>OTR<sub>interface</sub> (<math>\text{mg}\cdot\text{year}^{-1}</math>)</b>	<b>OTR<sub>stopper</sub>/OTR<sub>total</sub> (%)</b>
Agglomerated uncompressed stopper (interface glued)	$14.4 \pm 2$	$0.61 \pm 0.11$	/	/
Agglomerated compressed stopper (interface glued)	$9.2 \pm 2$	$0.38 \pm 0.08$	/	/
Agglomerated stopper compressed in a bottleneck without surface treatment	$130\,000 \pm 90\,000$	$17\,313 \pm 4432$	17 313	0.003
Agglomerated stopper compressed in a bottleneck with surface treatment	$7.9 \pm 2$	$0.34 \pm 0.08$	0	100

306  
 307 When the stopper is coated with a surface treatment agent, the effective oxygen diffusion  
 308 coefficients through 6 mm cork wafers compressed in a bottleneck were around  $8.8 \times 10^{-12} \text{ m}^2\cdot\text{s}^{-1}$ .  
 309 When extrapolated to a 48 mm cork stopper, the mean effective oxygen diffusion coefficient is  
 310  $7.9 \times 10^{-12} \text{ m}^2\cdot\text{s}^{-1}$ . This value is similar to that obtained previously for a compressed cork without  
 311 any transfer at the interface ( $9.2 \times 10^{-12} \text{ m}^2\cdot\text{s}^{-1}$ ). Moreover, the OTR at the interface between the

312 stopper and the bottleneck is around  $0.34 \text{ mg}\cdot\text{year}^{-1}$  compared with  $17\ 313 \text{ mg}\cdot\text{year}^{-1}$  in the case  
313 of a cork stopper compressed in a bottleneck without surface treatment. When coated with a  
314 surface treatment product, the oxygen flow at the interface decreases significantly and the  
315 effective diffusion coefficient becomes 10 000 times lower. These results emphasize the crucial  
316 role played by the surface treatment agent present between the stopper and the glass bottleneck  
317 on oxygen transfer. This thin layer coating appears to provide an efficient barrier against the  
318 ingress of oxygen from the external environment into the bottle. In addition to its primary  
319 function of facilitating uncorking, it can act as well as lubricating agent at bottling (during the  
320 compression and insertion stages) by reducing the creation of defects on the outer stopper  
321 surface. It can also act as an additional barrier to oxygen transfer by masking defects at the  
322 interface between the stopper and the bottleneck, providing an oxygen permeability as low as the  
323 cork stopper itself.

324

325 It should be noted that all analyses of oxygen transfer were performed under conditions that differ  
326 from oenological conditions (i.e., a dry sample under vacuum and without partial pressure of  
327 water and ethanol vapors). In a bottleneck, the cork is in contact with the wine (if bottles are  
328 stored horizontally) or in contact with a vapor phase saturated with water and ethanol vapors (if  
329 the bottles are stored vertically). These conditions might also affect the barrier properties of  
330 stopper. Further experiments are clearly needed to fully understand how the global diffusion  
331 coefficient of oxygen through cork could change depending on hydration or the presence of  
332 ethanol.

333

334 **4.3. Microscopic characterization of the surface coating**



335 In addition to permeability measurements, SEM analysis was performed for agglomerated  
336 stoppers with and without coating. The corresponding microscopic images of the cork stopper  
337 surface are presented in Figure 5. First, the stopper surface without coating is shown in Figure  
338 5A-B. The cork particles, as well as microspheres, are entrapped within the adhesive network that  
339 maintains the cohesion of the stopper. As the cork particles have no specific orientation, this  
340 confers more isotropy at the macroscopic scale, to the agglomerated stopper compared to the  
341 natural cork stopper having a strong anisotropy due to the specific orientation of cork cells  
342 (Gibson, Easterling & Ashby, 1981).

343 Surface treatment of the stopper, performed by drum coating with paraffin wax and silicone  
344 emulsion, results in a thin coating layer that can be observed on the stopper surface (Figures 5C-  
345 D). The deposited coating layer fully covers the surface of the stopper and does not tend to form  
346 aggregates (Fig 5C). It is also distributed in a very thin layer over the cork cells and does not fill  
347 the volume of the outer empty cells. Such SEM observation was performed at the scale of a 1  
348 mm<sup>2</sup> surface and is representative of the whole coated stopper surface. However, only small-scale  
349 observations could be performed with SEM microscopy. This method unfortunately does not  
350 enable a full assessment of the homogeneity of the coating on the surface of the whole stopper.  
351 Nevertheless, even if qualitative, these results seem to indicate that the coating was  
352 homogeneously distributed on the stopper surface, at the scale of observation provided by SEM.

353 At a lower scale, the coating thickness could be estimated from cross-sectional images at around  
354 0.5  $\mu\text{m}$  (Fig 5d) and was quite thin in view of the coating process. This thickness was much lower  
355 than the 17  $\mu\text{m}$  (paraffin wax layer) reported by Keenan *et al.* on natural cork stoppers (Keenan,  
356 Gozukara, Christie & Heyes, 1999). However, this last value was calculated from the weight and  
357 density of the paraffin. The weight value was obtained by solvent extraction of the wax layer

358 from cork stoppers. This result could thus be overestimated because of the solvent extraction of  
359 other compounds from the cork in addition to those used for the surface treatment.

360  
361

362

363

364

365

## 366 5. CONCLUSIONS

367

368 The transfer of oxygen in a cork/bottleneck system was assessed through a comprehensive study  
369 starting from the effective diffusion through the stopper alone and ending with a more complex  
370 system comprising the stopper covered by a surface treatment agent and compressed in the glass  
371 bottleneck. First, the effect of compression on agglomerated cork (with the interface glued)  
372 showed that a 40% reduction in the volume of the stopper (compression applied for still wines)  
373 reduced the effective oxygen diffusion of the stopper by 35%. Then, the oxygen transfer through  
374 a corked bottleneck was examined. Without coating, the oxygen effective diffusion coefficient  
375 through an agglomerated cork stopper compressed in a bottleneck was significantly higher than  
376 through the stopper alone ( $10^{-7} \text{ m}^2.\text{s}^{-1}$  vs  $10^{-11} \text{ m}^2.\text{s}^{-1}$ ). However, when the stopper was coated  
377 with a silicone-paraffin emulsion, the effective oxygen diffusion coefficient through the cork-  
378 bottleneck gave a similar value to that of the compressed stopper ( $10^{-11} \text{ m}^2.\text{s}^{-1}$ ). These results  
379 clearly highlighted the crucial role of the surface treatment in oxygen transfer through a corked  
380 bottleneck. A coating with a thickness of less than  $0.5 \mu\text{m}$  provided an efficient barrier for the  
381 stopper-bottleneck interface system to act against gas transfer at the interface. In addition to its

382 initial role of ensuring easier uncorking, the surface coating therefore confers an additional and  
383 unexpected barrier efficiency to the wine sealing system.

384

#### 385 AUTHOR CONTRIBUTIONS

386 T.K., J.C. and J.-P.B. designed research; T.K., R.D.G., J.C. and J.-P.B. performed research;  
387 T.K., J.C., R.D.G. and J.-P.B. analyzed data; and T.K., J.C., R.D.G., and J.-P.B. wrote the paper.

388

389

#### 390 ACKNOWLEDGMENTS

391 We gratefully acknowledge Diam Bouchage as well as the French National Association of  
392 Research and Technology (ANRT) for their financial support and the PhD grant (CIFRE 218-  
393 1278) of Julie Chanut. SEM images were determined at the Laboratoire Interdisciplinaire Carnot  
394 de Bourgogne with the help of Frédéric Herbst. We acknowledge the Bureau Interprofessionnel  
395 des Vins de Bourgogne for providing bottling machine and profilometer as well as Verrerie de  
396 Bourgogne for donating the bottles.

397

#### 398 COMPETING INTERESTS STATEMENT

399 The authors declare no competing interests.

400

401

402

403 REFERENCES

- 404
- 405 AFNOR. (2018). NF EN 12726 Emballage - Bague plate unique ayant un diamètre d'entrée de 18,5 mm  
406 pour bouchage liège et capsule témoin d'effraction. La Plaine Saint-Denis
- 407
- 408 Arapitsas, P., Speri, G., Angeli, A., Perenzoni, D. & Mattivi, F. (2014). The influence of storage on the  
409 "chemical age" of red wines. *Metabolomics*, 10, 816-832. <https://doi.org/10.1007/s11306-014-0638-x>
- 410
- 411 Caloghiris, M., Waters, E. J. & Williams, P. J. (1997). An industry trial provides further evidence for the  
412 role of corks in oxidative spoilage of bottled wines. *Australian Journal of Grape and Wine Research*, 3, 9-  
413 17. <https://doi.org/10.1111/j.1755-0238.1997.tb00110.x>
- 414
- 415 Chatonnet, P. & Labadie, D. (2003). Contrôle de la conformité des bouchons: objectifs et paramètres à  
416 l'usage des professionnels. *Revue française d'oenologie*, 198, 20-29.
- 417
- 418 Chevalier, V., Pons, A. & Loisel, C. (2019). Impact de l'obturateur sur le vieillissement des vins en  
419 bouteille Partie 1/3 – Caractérisation des transferts d'oxygène de bouchons en liège. *Revue des*  
420 *Oenologues*, 170, 40-43.
- 421
- 422 Crouvisier-Urien, K., Bellat, J.-P., Gougeon, R. D. & Karbowiak, T. (2018). Gas transfer through wine  
423 closures : A critical review. *Trends in Food Science & Technology*, 78, 255-269.  
424 <https://doi.org/10.1016/j.tifs.2018.05.021>
- 425
- 426 Crouvisier-Urien, K., Bellat, J.-P., Liger-Belair, G., Gougeon, R. & Karbowiak, T. (2020). Unravelling CO2  
427 transfer through cork stoppers for Champagne and sparkling wines. *Food Packaging and Shelf Life*, *In*  
428 *Press*.
- 429
- 430 Fortes, M. A., Rosa, M. E. & Pereira, H. (2004). *A Cortiça*. I. Press, Lisboa
- 431
- 432 Gibson, L. J., Easterling, K. E. & Ashby, M. F. (1981). The structure and mechanics of cork *Proceedings of*  
433 *the Royal Society of London*, 377, 99-117. <https://doi.org/10.1098/rspa.1981.0117>
- 434
- 435 Gonzalez-Adrados, J. R., Garcia-Vallejo, M. C., Caceres-Esteban, M. J., Garcia de Ceca, J. L., Gonzalez-  
436 Hernandez, F. & Calvo-Haro, R. (2011). Control by ATR-FTIR of surface treatment of cork stoppers and its  
437 effect on their mechanical performance. *Wood Science and Technology*, 46, 349-360.  
438 <https://doi.org/10.1007/s00226-011-0403-5>
- 439
- 440 Gonzalez-Adrados, J. R., Gonzalez-Hernandez, F., Garcia de Ceca, J. L., Caceres-Esteban, M. J. & Garcia-  
441 Vallejo, M. C. (2008). Cork-Wine Interaction studies : Liquid absorption and non-volatile compound  
442 migration *J. Int. Sci. Vigne Vin*, 42, 161-166. <https://doi.org/10.20870/oeno-one.2008.42.3.815>
- 443
- 444 Karbowiak, T., Crouvisier-Urien, K., Lagorce, A., Ballester, J., Geoffroy, A., Roullier-Gall, C., Chanut, J.,  
445 Gougeon, R. D., Schmitt-Kopplin, P. & Bellat, J.-P. (2019). Wine aging: a bottleneck story. *Npj Science of*  
446 *Food*, 14, <https://doi.org/10.1038/s41538-019-0045-9>
- 447

448 Karbowski, T., Gougeon, R. D., Alinc, J.-B., Brachais, L., Debeaufort, F., Voilley, A. & Chassagne, D. (2010).  
449 Wine oxidation and the role of cork. *Critical Reviews in Food Science and Nutrition*, 50, 20-52.  
450 <https://doi.org/10.1080/10408398.2010.526854>  
451 Keenan, C. P., Gozukara, M. Y., Christie, G. B. Y. & Heyes, D. N. (1999). Oxygen permeability of  
452 macrocrystalline paraffin wax and relevance to wax coatings on natural corks used as wine bottle  
453 closures. *Australian Journal of Grape and Wine Research*, 5, 66-70. <https://doi.org/10.1111/j.1755-0238.1999.tb00154.x>  
454  
455 Lagorce-Tachon, A., Karbowski, T., Paulin, C., Simon, J.-M., Gougeon, R. D. & Bellat, J.-P. (2016). About  
456 the role of the bottleneck/cork interface on oxygen transfer. *Journal of Agricultural and Food Chemistry*,  
457 64, 6672-6675. <https://doi.org/10.1021/acs.jafc.6b02465>  
458  
459 Lagorce-Tachon, A., Karbowski, T., Simon, J.-M., Gougeon, R. D. & Bellat, J.-P. (2014). Diffusion of oxygen  
460 through cork stopper: Is it a Knudsen or a Fickian mechanism? *Journal of Agricultural and Food*  
461 *Chemistry*, 62, 9180-9185. <https://doi.org/10.1021/jf501918n>  
462  
463 Lefebvre, A., Riboulet, J.-M., Alegoet, C., Pouillaude, C., Lacorne, F. & Natividade, J. V. (2006). Charte des  
464 bouchonniers liègeurs. Paris, France  
465  
466 Lequin, S., Chassagne, D., Karbowski, T., Simon, J.-M., Paulin, C. & Bellat, J.-P. (2012). Diffusion of oxygen  
467 in cork. *Journal of Agricultural and Food Chemistry*, 60, 3348-3356. <https://doi.org/10.1021/jf204655c>  
468  
469 Lopes, P., Saucier, C., Teissedre, P.-L. & Glories, Y. (2006). Impact of storage position on oxygen ingress  
470 through different closures into wine bottles. *Journal of Agricultural and Food Chemistry*, 54, 6741-6746.  
471 <https://doi.org/10.1021/jf0614239>  
472  
473 Lopes, P., Saucier, C., Teissedre, P.-L. & Glories, Y. (2007a). Main Routes of oxygen ingress through  
474 different closures into wine bottles. *Journal of Agricultural and Food Chemistry*, 55, 5167-5170.  
475 <https://doi.org/10.1021/jf0706023>  
476  
477 Lopes, P., Saucier, C., Teissedre, P.-L. & Glories, Y. (2007b). Oxygen transmission through different  
478 closures into wine bottles. *Practical Winery & Vineyard*  
479  
480 Lopes, P., Silva, M. A., Pons, A., Tominaga, T., Lavigne, V., Saucier, C., Darriet, P., Cabral, M., Teissedre, P.-  
481 L. & Dubourdieu, D. (2012). Impact of the Oxygen Exposure during Bottling and Oxygen Barrier  
482 Properties of Different Closures on Wine Quality during Post-Bottling. in: *Flavor Chemistry of Wine and*  
483 *Other Alcoholic Beverages* (pp. 167-187)  
484  
485 Rabiot, D., Sanchez, J. & Aracil, J. M. (1999). Study of the oxygen transfer through synthetic corks for  
486 wine conservation. *Second European congress of chemical engineering*, Montpellier, France  
487  
488 Roullier-Gall, C., Hemmler, D., Gonsior, M., Li, Y., Nikolantonaki, M., Aron, A., Coelho, C., Gougeon, R. D.  
489 & Schmitt-Kopplin, P. (2017). Sulfites and the wine metabolome. *Food Chemistry*, 237, 106-113.  
490 <https://doi.org/10.1016/j.foodchem.2017.05.039>  
491  
492 Roullier-Gall, C., Witting, M., Moritz, F., Schmitt-Kopplin, P. & Gougeon, R. (2016). Natural oxygenation  
493 of Champagne wine during the prise de mousse: a metabolomics picture of hormesis. *Food Chemistry*,  
494 203, 207-215. <https://doi.org/10.1016/j.foodchem.2016.02.043>  
495

496  
497 Venturi, F., Sanmartin, C., Taglieri, I., Xiaoguo, Y., Andrich, G. & Zinnai, A. (2016). The influence of  
498 packaging on the sensorial evolution of white wine as a function of the operating conditions adopted  
499 during storage. *Agrochimica*, 60, 150-159. <https://doi.org/10.12871/0021857201627>  
500  
501 Waters, E. J. (1997). Random post-bottling oxidation of bottled wines. *Australian Grapepower and*  
502 *Winemaker*, 408, 46-47.  
503  
504 Waters, E. J., Peng, Z., Pocock, K. F. & Williams, P. J. (1996). The role of corks in oxidative spoilage of  
505 white wines. *Australian Journal of Grape and Wine Research*, 191-197. [https://doi.org/10.1111/j.1755-](https://doi.org/10.1111/j.1755-0238.1996.tb00108.x)  
506 [0238.1996.tb00108.x](https://doi.org/10.1111/j.1755-0238.1996.tb00108.x)  
507  
508 Waters, E. J., Skouroumounis, G., Sefton, M. A., Francis, I. L., Peng, Z. K. & Kwiatkowski, M. (2001). The  
509 inherent permeability of corks to oxygen *Australian Wine Institut 46<sup>th</sup> Annual Report*, 31  
  
510

**Figure 1.** Conditions used for the measurement of oxygen transfer.

**Figure 2.** Scheme of the homemade manometric device for the oxygen transfer measurement of the different cork samples

**Figure 3.** Experimental and extrapolated distributions of the logarithm of the diffusion coefficient of oxygen of uncompressed and compressed agglomerated cork stoppers at 298 K obtained from 10 replicates. Green dashed line (---): experimental distribution of a 3 mm uncompressed cork wafer. Blue dashed line (---): experimental distribution of a 6 mm compressed cork wafer (from 10 replicates). Green line (-): extrapolated distribution to a 48 mm stopper from the experimental data measured for 3 mm uncompressed cork wafers. Blue line (-): extrapolated distribution to a 48 mm stopper from the experimental data measured for 6 mm compressed cork wafers.

**Figure 4.** Distributions of the logarithm of the diffusion coefficient of oxygen at 298 K obtained from 10 replicates. Green (-): extrapolated distribution to a 48 mm stopper from the experimental data for 3 mm compressed cork wafers. Blue (-): extrapolated distribution to a 48 mm stopper from the experimental data for 6 mm compressed cork wafers. Red (-): experimental distribution of 48 mm stoppers compressed in a bottleneck without surface treatment. Yellow (-): extrapolated distribution to 48 mm stoppers from the experimental data measured for 6 mm cork wafers compressed in a bottleneck with surface treatment (emulsion of paraffin and silicone).

**Figure 5.** SEM observations of the surface of agglomerated stoppers observed at different magnifications factors. a) without surface treatment, b) cross section of agglomerated cork stopper without surface treatment c) with surface treatment, d) cross section of an agglomerated cork stopper with surface treatment.

**Table 1.** Mean oxygen diffusion coefficients and OTRs determined for uncompressed and compressed cork stoppers alone and for cork stoppers inserted in a bottleneck with and without a surface treatment agent (extrapolated to a full cork stopper, from 10 replicates in each case; see figure 4 for corresponding distributions). For practical reasons, OTR is expressed as  $\text{mg}\cdot\text{year}^{-1}$ , referring to as mg of oxygen going through the stopper per year.

Figure 1

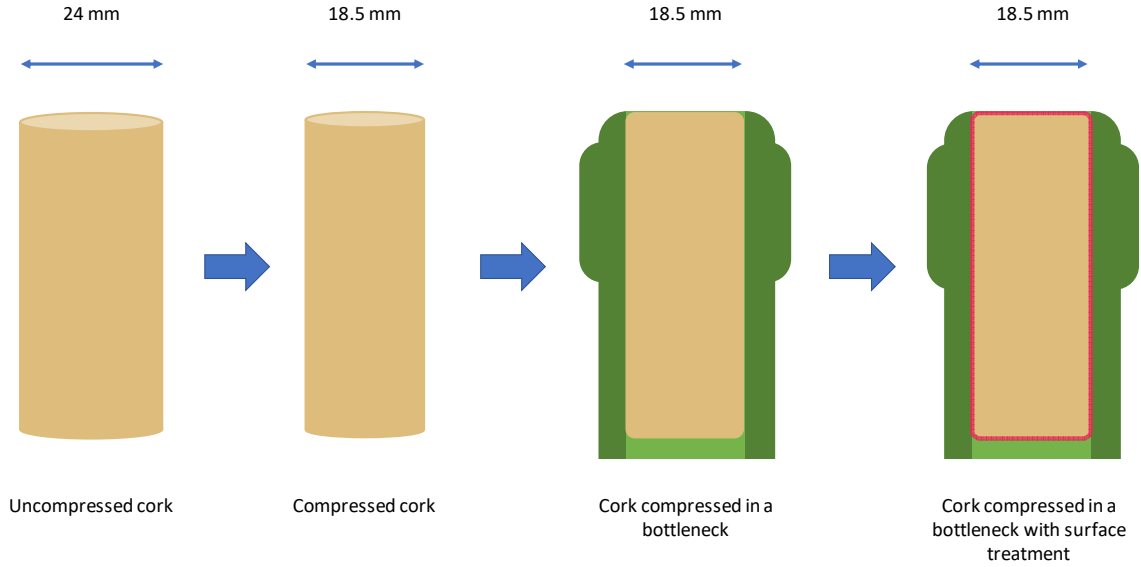




Figure 2

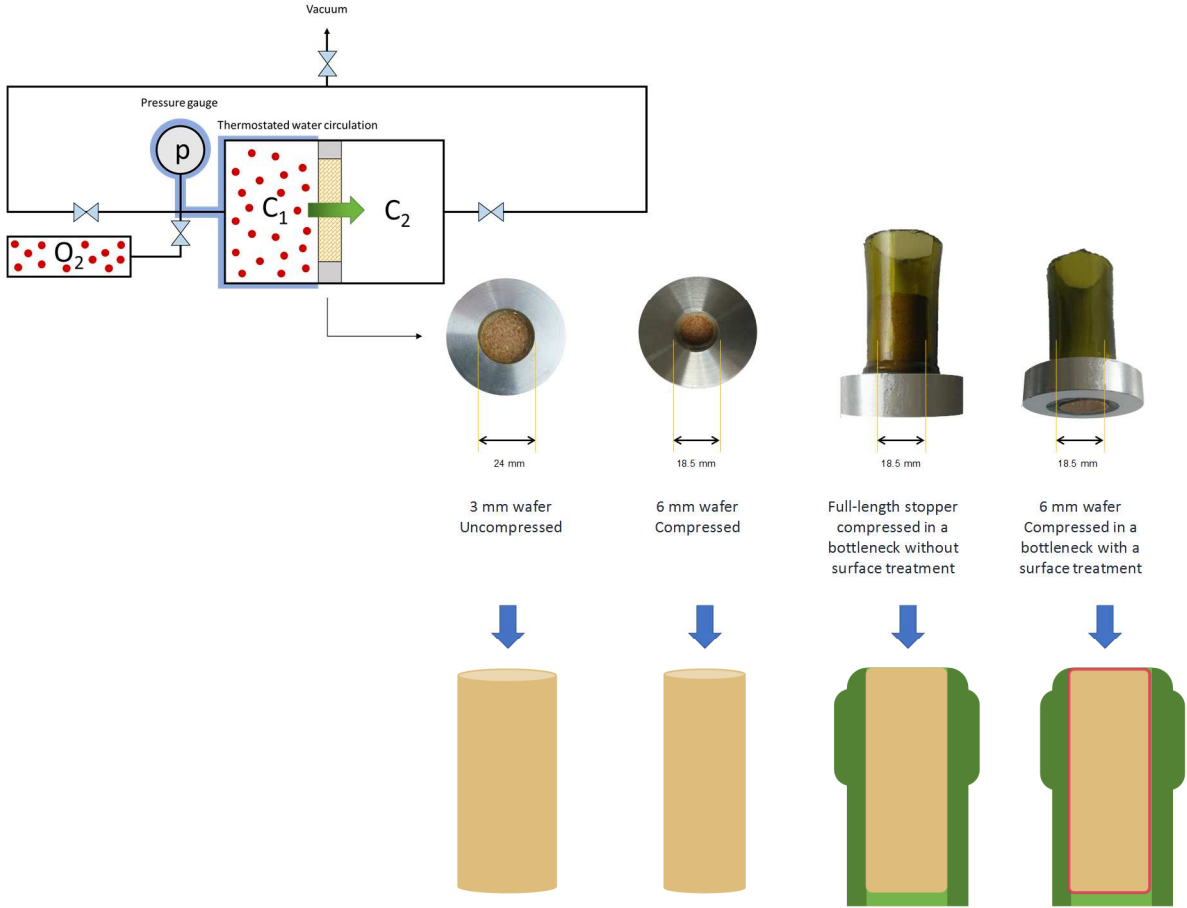


Figure 3

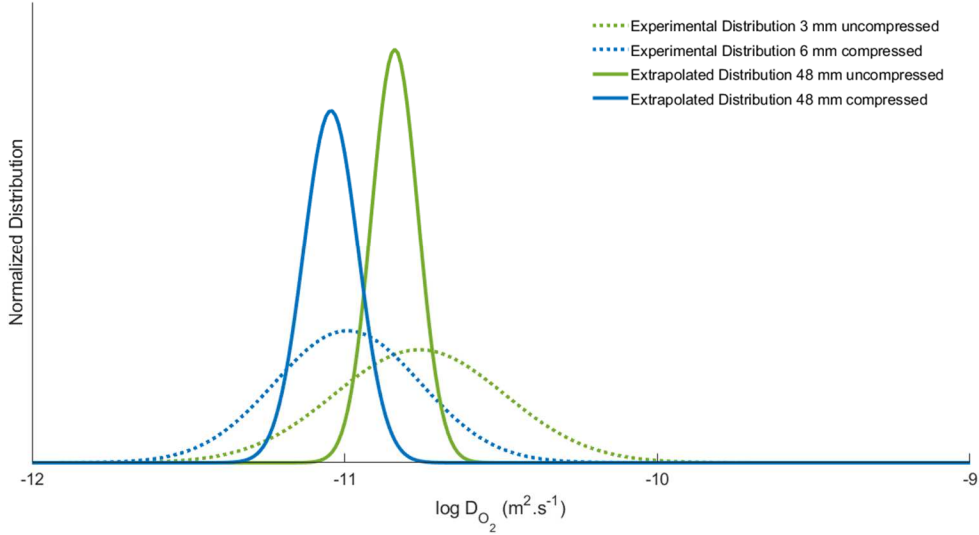


Figure 4

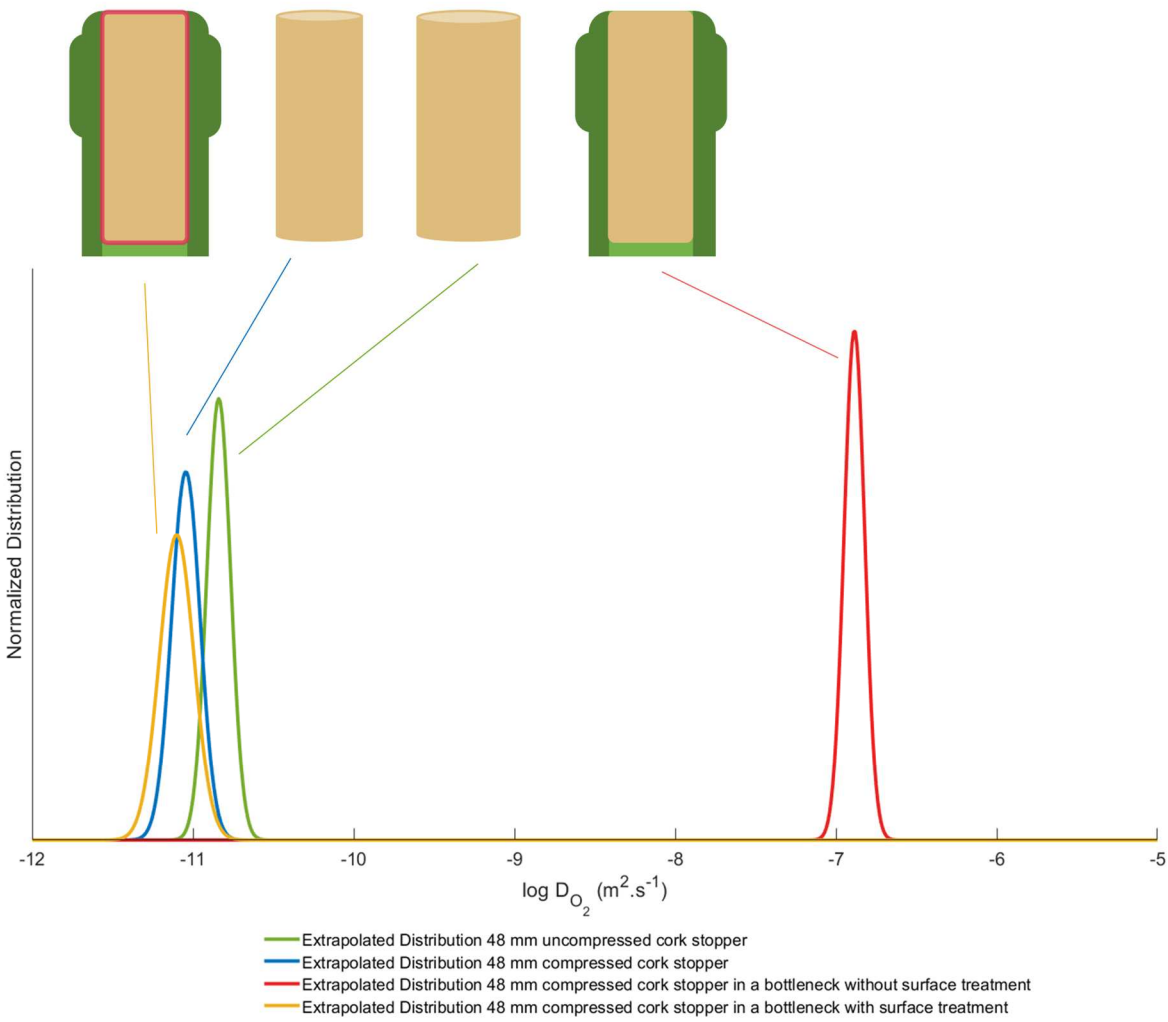
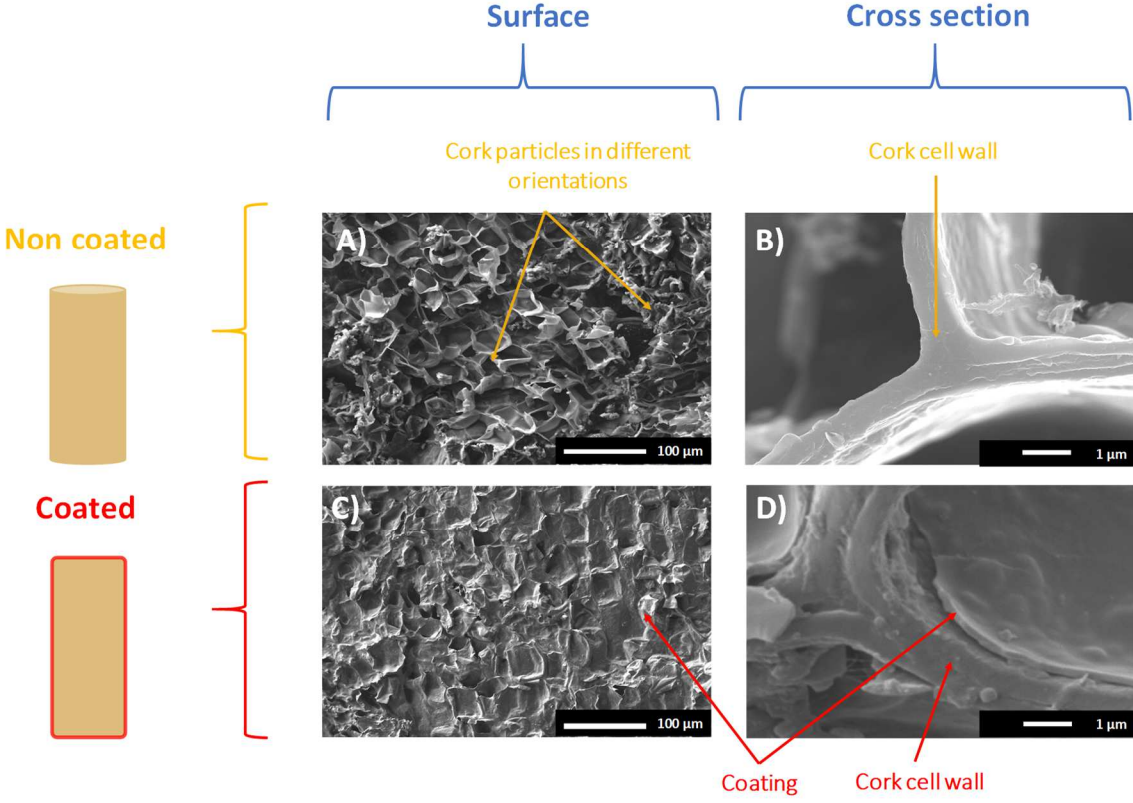


Figure 5



# Graphical abstract

